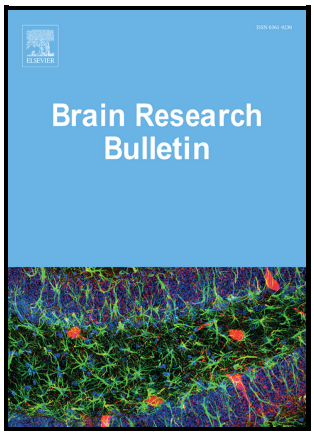
Journal Pre-proof

Terahertz Radiation Affects the Dynamics of Neurons by Decreasing Membrane Area Ratio

Shaoqing Ma, Siyu Li, Huan Wang, Yingwei Li, Chengbiao Lu, Xiaoli Li



PII: S0361-9230(25)00185-6

DOI: https://doi.org/10.1016/j.brainresbull.2025.111373

Reference: BRB111373

To appear in: *Brain Research Bulletin*

Received date: 23 December 2024
Revised date: 10 April 2025
Accepted date: 4 May 2025

Please cite this article as: Shaoqing Ma, Siyu Li, Huan Wang, Yingwei Li, Chengbiao Lu and Xiaoli Li, Terahertz Radiation Affects the Dynamics of Neurons by Decreasing Membrane Area Ratio, *Brain Research Bulletin,* (2025) doi:https://doi.org/10.1016/j.brainresbull.2025.111373

This is a PDF file of an article that has undergone enhancements after acceptance, such as the addition of a cover page and metadata, and formatting for readability, but it is not yet the definitive version of record. This version will undergo additional copyediting, typesetting and review before it is published in its final form, but we are providing this version to give early visibility of the article. Please note that, during the production process, errors may be discovered which could affect the content, and all legal disclaimers that apply to the journal pertain.

© 2025 Published by Elsevier Inc.

Terahertz Radiation Affects the Dynamics of Neurons by Decreasing Membrane Area Ratio

Shaoqing Ma[1,2,3], Siyu Li[4], Huan Wang[5], Yingwei Li[2,3*], Chengbiao Lu[6*], Xiaoli Li[7,8*]

[1] School of Management Science and Information Engineering, Hebei University of Economics and Business, Shijiazhuang 050062, China.
[2] School of Information Science and Engineering, Yanshan University, Qinhuangdao 066004, China.
[3] Hebei Key Laboratory of Information Transmission and Signal Processing, Qinhuangdao 066004, China.
[4] School of Electronic and Information Engineering, Hebei University of Technology, Tianjin 300401, China.
[5] School of Electrical Engineering, Beijing Jiaotong University, Beijing 100044, China.
[6] Henan International Key Laboratory for noninvasive Neuromodulation, Xinxiang Medical University, Xinxiang 453003, China.
[7] School of Automation Science and Engineering, South China University of Technology, Guangzhou 510641, China.
[8] Pazhou Lab, Guangzhou 510330, China.

*Address correspondence to: Yingwei Li, lyw@ysu.edu.cn; Chengbiao Lu, johnlu9000@163.com; Xiaoli Li, xiaolili@scut.edu.cn.

Yingwei Li will answer any future questions about your results, data, methods and materials

Journal Pre-proof

Abstract

Terahertz radiation at specific frequencies and energies can mediate cellular morphology or function changes by exciting nonlinear resonance effects in proteins or DNA. However, the effects of terahertz radiation on neuronal morphology and function are currently unknown, and the correlation between neuronal morphology and kinetic properties after terahertz radiation remains to be elucidated. In this paper, we first characterized the changes in neuronal morphology by the relative ratio of neuronal cytosol to protruding membrane area. Analyzed the pattern of the influence of terahertz radiation on neuronal morphology and the cumulative effect. On this basis, this paper constructs a kinetic model of neurons regulated by terahertz radiation, investigates the influence law of terahertz radiation on the kinetic properties of neurons, and analyzes the correlation between neuronal morphology and kinetic properties. The results showed that terahertz radiation caused a decrease in the membrane area ratio of neuronal cytosol to protrusion, and this effect started on the first day of terahertz radiation and lasted until the end of terahertz radiation; terahertz radiation changed the neuronal discharge pattern by decreasing the membrane area ratio of neuronal cytosol to protrusion and lowered the frequency of neuronal inter-cluster discharges and amplitude of action potentials, and increased the neuronal intra-cluster discharge. In addition, terahertz radiation can increase the peak value of neuronal postsynaptic currents by decreasing the membrane area ratio. In summary, terahertz radiation can modulate neurons' morphology and change their firing patterns and kinetic properties by affecting their morphology. These predict that terahertz radiation at specific

frequencies and energies can be developed as a novel, molecular-level neuromodulation technique for intervening or treating neuronal degenerative diseases.

Keywords: Terahertz Radiation, Neurons, Neuronal Dynamics, Neuronal Morphology, Synaptic Transmission

INTRODUCTION

Terahertz radiation is an electromagnetic wave between microwave and infrared light waves with a frequency of 0.1-10 THz[1,2]. Many biomolecules interact with energy levels located in the terahertz band, where absorption and resonance are strong [3], which means that even simple molecules can absorb terahertz radiation well[4]. In addition, low-frequency terahertz vibrations are prevalent in living organisms[5], and the function of life is closely related to low-frequency terahertz vibrations. Changes in terahertz dynamics determine functional states, such as ion transport and ligand binding[6,7], and manipulation of low-frequency vibrations in living organisms can influence functional states in living systems[8,9]. Although the energy of terahertz radiation is not sufficient to break chemical bonds between molecules, theory, and experiments have shown that terahertz radiation can interact with hydrogen bonds in proteins, causing low-frequency molecular vibrations, which can lead to changes in the conformational and functional properties of proteins[10-12]. Thus, terahertz radiation can mediate cellular structure and function changes by exciting nonlinear resonance effects in proteins and DNA. Based on this mechanism, terahertz radiation of specific frequency and energy can modulate neuronal morphology and function at the molecular level.

Several studies have shown that terahertz radiation can affect the morphological and kinetic properties of neurons[13-16] and that higher terahertz radiation power (0.12 THz, 10 mW; 0.157 THz, 50 mW) leads to neuronal apoptosis with mitochondrial damage and increased lysosomes [17]. To reduce the damage to neurons by terahertz radiation, some studies have chosen to reduce the terahertz radiation power and shorten the radiation time. For example, Sulatsky et al. used terahertz radiation (0.1-2 THz) on spinal cord neurons of chicken embryos for 3 and 5 min. When the terahertz power density was reduced to 19 mW/cm^2, the neuronal growth in the radiation group increased by 118.76 ± 11.3% compared to the control group[18]. Even more amazingly, neuronal growth can still be promoted using μW levels of terahertz radiation[19,20]. Studies in neuronal kinetic properties have shown that terahertz radiation increases the rate of Ca^{2+} through ion channels[21]and that terahertz radiation (0.094 THz, 60 mW) also increases the number of peaks and spikes of Ca^{2+} in neurons[22,23]. Zhang et al. from Tianjin University conducted further research on this basis. They found that Ca^{2+} and Na^{+} concentrations were elevated, and K^{+} concentration was decreased in neurons after radiation[24]. In addition, terahertz radiation enhances excitatory synaptic transmission and neuronal firing rate in neurons[25]. Many experimental and modeling studies have shown that neuronal morphology can influence neuronal discharge properties[26,27], and therefore, changes in neural discharge properties are usually accompanied by changes in neuronal morphology. Investigating the pattern of terahertz radiation effects on neuronal morphological parameters (membrane area of cytosol and protrusion) is crucial for understanding the relationship between neuronal structure and kinetic properties.

Neurons are essential components of neural networks, and neuronal morphology influences the way they receive and transmit information[28], in which neuronal cytosol and protrusions function to receive and integrate afferent information from neighboring neurons, and the diversity of their morphology facilitates both local and remote signaling. Neuronal morphology also has an essential effect on electrical signaling, and the membrane area ratio of neuronal cytosol and protrusions is known to be highly correlated with the

Journal Pre-proof

discharge electrodynamic properties of neurons based on the equivalent cable model of neurons[29]. Numerous experimental and modeling studies have shown that neuronal morphology can influence the function of neurons and nerve clusters[30,31]. In addition, Pinsky and Rinzel developed neuronal models that can simulate the firing pattern of CA3 pyramidal neurons, in which the firing properties of neurons are highly correlated with the membrane area ratio between neuronal cytosol and protrusion[32]. Therefore, the membrane area ratio of cytosol to protrusion in neurons can be used as a neuromodulatory factor to influence the firing characteristics of neurons. However, the regulation pattern of neuronal morphology (membrane area of cytosol and protrusion) by short-term cumulative terahertz radiation is not clear, and the long-term effect of terahertz radiation on neuronal morphology is not known yet, as the change of neuronal morphology is a dynamic and continuous process. In addition, the correlation between neuronal morphology and discharge properties after terahertz radiation remains to be elucidated.

This paper first investigated the effect of short-time cumulative terahertz radiation (0.138 THz, maximum radiation power 2 mW, 20 min/day for 3 days) on neuronal morphology. A terahertz radiation system compatible with neuronal morphology recording was built into the study, and the dynamic changes of neuronal morphology were recorded in real time. The changes in neuronal morphology were characterized by the neuronal cytosolic membrane area, the protruding membrane area, and the area ratio of the two, and the influence pattern and cumulative effect of 0.138 THz radiation on neuronal morphology were analyzed. On this basis, the correlation between neuronal morphology and discharge characteristics after terahertz radiation was further investigated. In the study, the membrane area ratio of cytosol and protrusion in neurons was taken as the regulatory factor of neuronal discharge regulated by terahertz radiation. The influence law of terahertz radiation on neuronal discharge characteristics was investigated, and the correlation between terahertz radiation time and discharge characteristics was analyzed.

RESULTS

Terahertz radiation decreases the ratio of membrane area of neuronal cytosol to protrusion

Neuronal morphology has an essential influence on the conduction of electrical signals, and the membrane area ratio of neuronal cytosol and dendrites is known to be highly correlated with the exergonic mechanical properties of neurons according to the equivalent cable model of neurons[33]. Therefore, the effect of terahertz radiation on the membrane area ratio of neuronal cytosol and dendrite was investigated. Narrowband high-power terahertz waves were used to radiate the neurons for 20 min/day for 3 days, and the patterns of change in the membrane area ratio of neuronal cytosol and dendrites were statistically analyzed for the initial state and the 3 days of radiation, respectively, as shown in Fig.1. Where Fig.1(A) is a representative neuronal image that gives the dynamic changes in neuronal morphology before terahertz radiation and within 1-3 days of terahertz radiation. Before terahertz radiation neurons in both the control and terahertz groups had grown appositionally and had a few protrusions. Within 1-3 days of terahertz radiation neuronal cytosol and protrusion changes were evident and well developed.

As shown in Figure 1(B), neurons were divided into control (CON) and terahertz (THz) groups before terahertz radiation, and significant differences between the two groups were analyzed to highlight the effect of terahertz radiation on the membrane area ratio of neurons. Where CON was not exposed to terahertz radiation, THz was subjected to 3 days of terahertz radiation (20 min/day). In order to minimize the difference between the membrane area proportions of neurons in the two groups before terahertz radiation and to highlight the effect of terahertz stimulation on the membrane area proportions of neurons, the difference between THz and CON before terahertz radiation was statistically analyzed. It was found

Journal Pre-proof

that there was no significant difference in the membrane area ratio between the cytosol and protrusion of THz and CON neurons before terahertz radiation. However, after 1 day of terahertz radiation, the membrane area ratios of cytosol and protrusion of neurons in the terahertz group were significantly lower than those in the control group. Further, an increase in the duration of terahertz radiation revealed that the membrane area ratios of cytosol and protrusion of neurons in the terahertz group were significantly lower than those of the control group on days 2 and 3 of terahertz radiation. Subsequently, the relationship between neuronal cytosol's membrane area ratios and protrusion and terahertz radiation's time was further statistically analyzed, as shown in Fig.1(C). The membrane area ratios of neuronal cytosol and protrusion were significantly lower than the initial state on day 1 of terahertz radiation. They were lower than the initial state on days 2 and 3 of radiation. However, there was no significant difference in the membrane area ratio between days 1 and 2, and between days 2 and 3 of terahertz radiation.

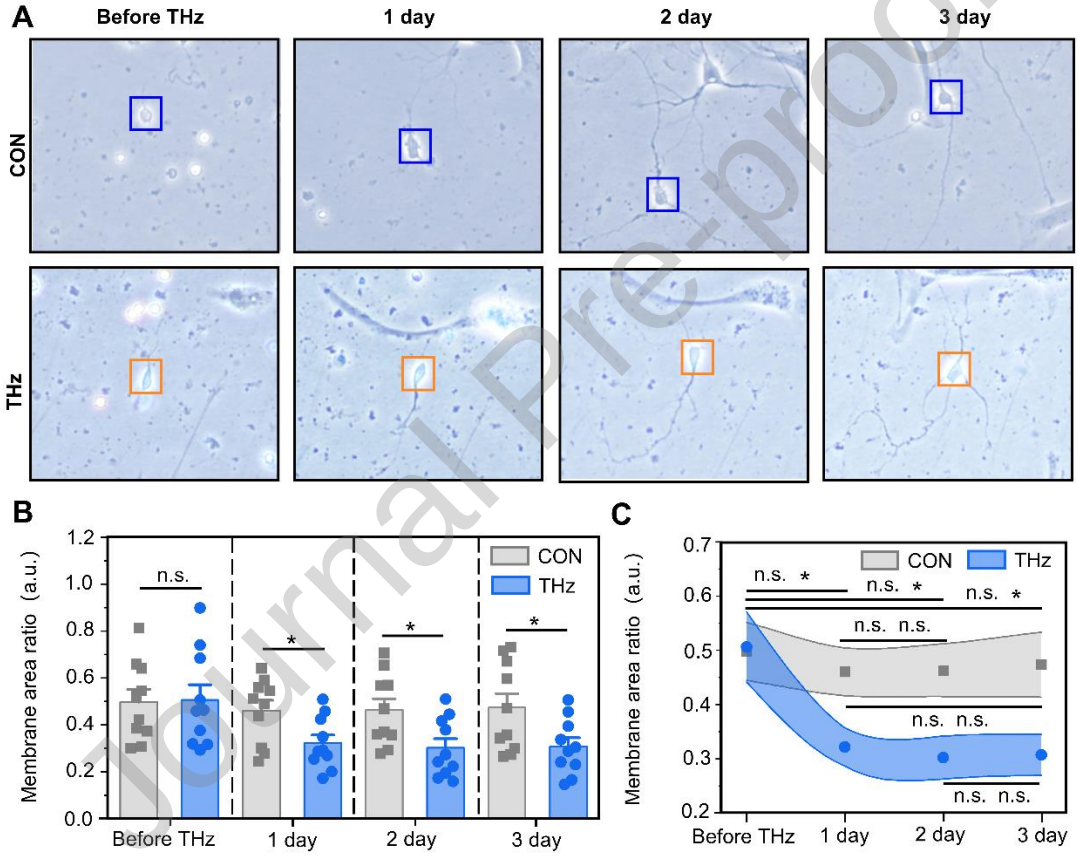


Fig.1. Effect of terahertz radiation on the ratio of neuronal cytosol to protruding membrane area. (A) Changing the law of neuronal cytosol to protrusion membrane area ratio in the terahertz and control groups. (B) Patterns of change in the ratio of neuronal cytosol to protruding membrane area with time of terahertz radiation. (Gray indicates the the control group (CON) and blue indicates the terahertz group (THz), All data shown as means ± SEM, *P<0.05) ns, not significant.

Terahertz radiation can affect neuronal discharge dynamics properties

In studying the effect of narrow-band terahertz radiation on the kinetic properties of neurons, we coupled the computed neuronal morphology parameter p to intercompartment cone neuron model. Since the parameter p is calculated based on the morphology of neurons after terahertz radiation, the parameter p is with terahertz radiation properties. By coupling the parameter p into the neuron model, the neuron discharge properties and the change rule of postsynaptic current after terahertz radiation can be obtained. It was found that the control group had periodic bimodal discharges on the first day of terahertz radiation, whereas the terahertz group had periodic 3-peak discharges. On days 2 and 3 of terahertz radiation, the

Journal Pre-proof

control group had periodic bimodal discharges, whereas the terahertz group had 4-peak and 3-peak discharges, respectively, as shown in Fig.2(A).

The effects of narrow-band high-power terahertz radiation on neuronal inter-cluster and intra-cluster discharge frequencies, action potential amplitudes, slopes, and decline times were statistically analyzed in Fig.2(B) for different days of terahertz radiation.

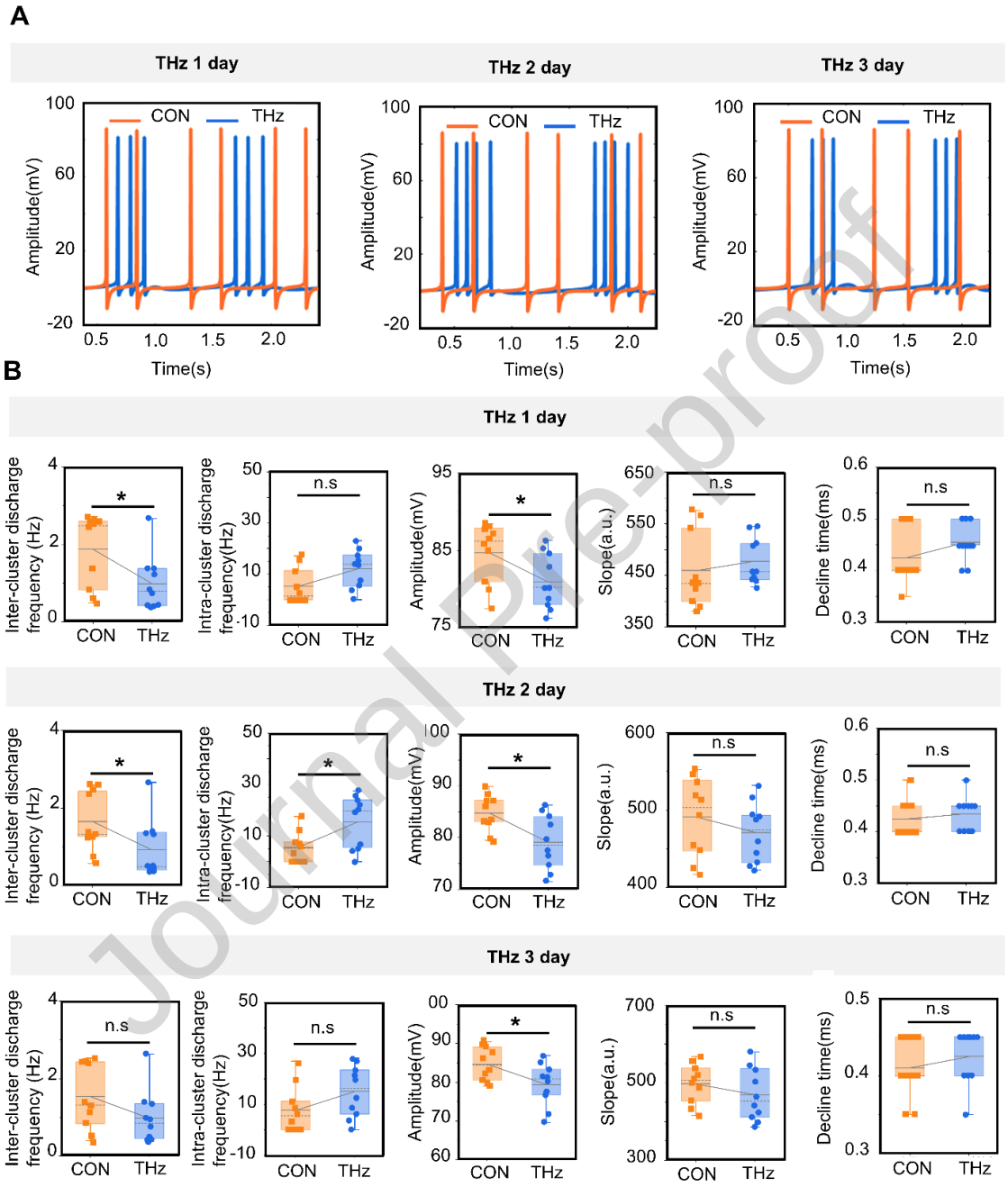


Fig.2. The effect of terahertz radiation on the electrodynamic properties of neuronal discharge. (A) Changes in neuronal cytosolic membrane potential after terahertz radiation. (B) The effect of terahertz radiation on the frequency of inter- and intra-cluster neuronal discharges, action potential amplitude, slope, and fall time. (All data shown as means±SEM,*P<0.05) ns, not significant.

On the first day of terahertz radiation, the inter-cluster discharge frequency of neurons was significantly lower than that of the control group, and the action potential amplitude of neurons was also significantly lower than that of the control group; further analysis revealed that the intra-cluster discharge frequency, the slope of action potentials, and the decline time of neurons after terahertz radiation were not significantly different from those of the control group. On the second day of the radiation, the discharge frequency and the amplitude of

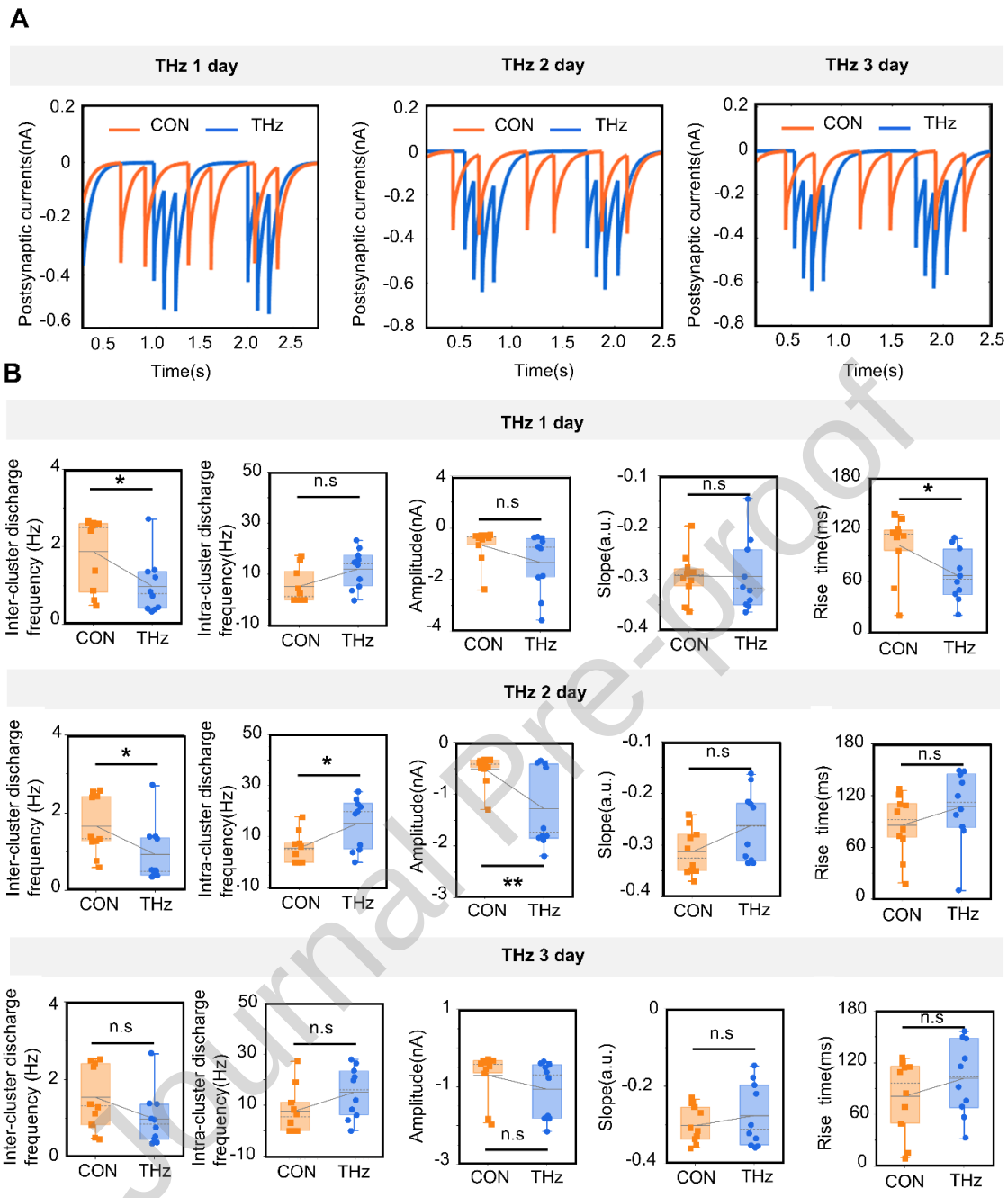
Journal Pre-proof

action potentials between clusters of neurons were significantly lower than those of the control group. The discharge frequency within clusters was significantly higher than that of the control group. However, the decline in the time of action potentials of neurons was not significantly different from that of the control group. A different phenomenon was found on day 3 of terahertz radiation. The frequency of inter-cluster and intra-cluster discharges of neurons after terahertz radiation was not significantly different from that of the control group, and there were no significant differences in the amplitude and fall time of action potentials. However, the amplitude of action potentials was significantly lower than that of the control group.

Terahertz radiation can affect the properties of neuronal synaptic transmission dynamics

The postsynaptic current of neurons is also a heavy route for neurons to transmit information, so the law of the effect of narrow-band high-power terahertz radiation on the postsynaptic current of neurons was analyzed, as shown in Fig. 6. From Fig.3(A), it was found that on days 1 to 3 of terahertz radiation the postsynaptic currents of the control neurons showed periodic bimodal discharges. In contrast, the terahertz group had 3-peak discharges on day 1 and periodic 4-peak discharges on days 2 and 3.

Journal Pre-proof



Journal Pre-proof

Fig.3. Effects of terahertz radiation on the kinetic properties of synaptic transmission in neurons. (A) Postsynaptic current changes in neurons after terahertz radiation. (B) Effect of terahertz radiation on the frequency, amplitude, slope, and rise time of inter- and intra-cluster generation of postsynaptic currents. (All data shown as means±SEM,*P<0.05) ns, not significant.

In order to study in more detail the effects of narrow-band high-power terahertz radiation on the kinetic parameters of neuronal postsynaptic currents, the effects of narrow-band high-power terahertz radiation on the frequency, amplitude, slope, and rise time of inter- and intra-cluster generation of neuronal postsynaptic currents were analyzed statistically for different days of terahertz radiation, respectively, as shown in Fig.3(B). On day 1 of terahertz radiation, the frequency of inter-cluster generation of postsynaptic currents was significantly lower than that of the control group, and the rise time of postsynaptic currents was also significantly lower than that of the control group. However, the amplitude, slope, and frequency of intra-cluster generation postsynaptic currents in neurons after terahertz radiation were not significantly different from those in the control

group. On the second day of terahertz radiation, the frequency and amplitude of inter-cluster generation of neuronal postsynaptic currents were significantly lower than those of the control group. Further analysis revealed that the frequency of intra-cluster generation of neuronal postsynaptic currents in the terahertz group was higher than that of the control group. However, there was no significant difference in the slope and the rise time of the neuronal postsynaptic currents with that of the control group. Moreover, there was no significant change in neuronal postsynaptic kinetic parameters on the third day of radiation.

To further investigate the correlation between terahertz radiation time and neuronal kinetic properties, the changing patterns between the number of radiation days and neuronal kinetic parameters were analyzed, as shown in Figure 4. From Fig.4(A), it can be found that there is no significant relationship between the inter-cluster discharge frequency, action potential amplitude, and rise time of neurons in the control and terahertz groups with the number of terahertz radiation days. From Fig.4(B), it can be found that the frequency, amplitude, and fall time of inter-cluster generation of postsynaptic currents in neurons of the control and terahertz groups were also not significantly related to the number of terahertz radiation days. These phenomena indicate that most of the kinetic parameters of the neurons changed independently of the number of terahertz radiation days.

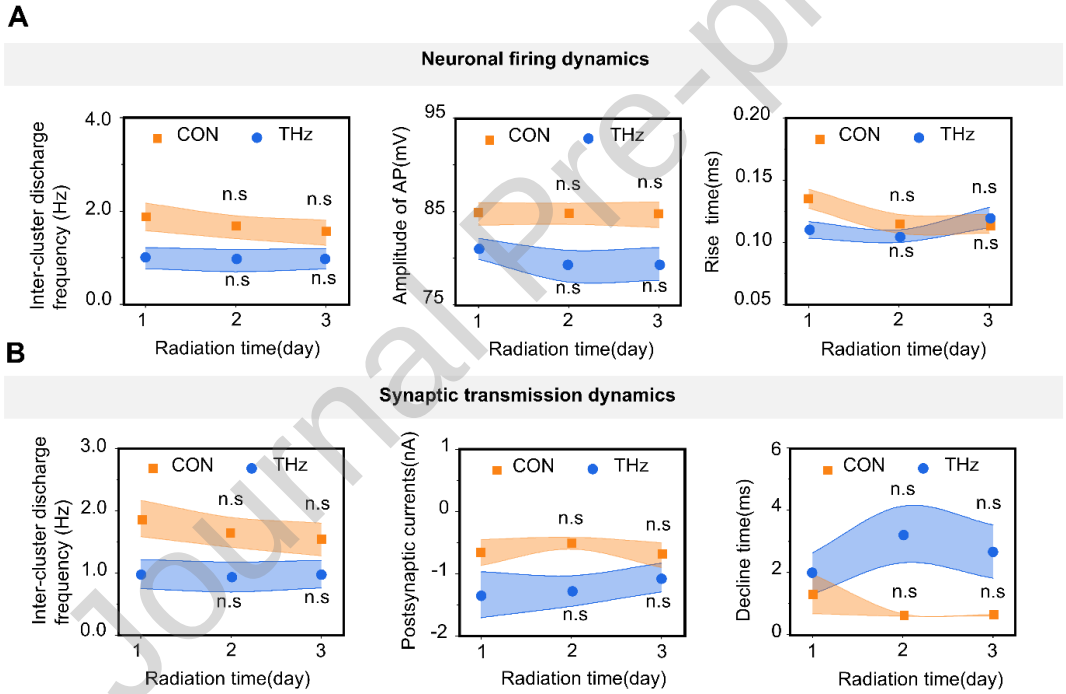


Fig.4. Correlation of terahertz radiation duration with neuronal kinetic properties. (A) Variation of neuronal electrodynamic properties with time of terahertz radiation. (B) Variation of neuronal synaptic transmission kinetic properties with time of terahertz radiation. (All data shown as means±SEM,*P<0.05) ns, not significant.

DISCUSSION and CONCLUSION

In The present study found that terahertz radiation causes a decrease in the neuronal cytosol to protrusion membrane area ratio and that this effect begins on day 1 of radiation and continues until the end of terahertz radiation (day 3). However, the change in the neuronal cytosol to protrusion membrane area ratio differs in the neuronal cytosol to protrusion growth cycle. Where neuronal growth and development is a dynamic process, based on the developmental cycle of in vitro cultured neurons, it is known that neuronal protrusions are in a period of rapid growth within 1-3 days of terahertz radiation [34]. Moreover, previous studies have shown that terahertz radiation promotes neuronal cytosol and protrusion growth, while there is a cumulative effect on promoting neuronal protrusions [14,16]. These reasons lead to a higher rate of neuronal protrusion growth than neuronal

Journal Pre-proof

cytosol growth during terahertz radiation. So, terahertz radiation causes a decrease in the membrane area ratio of neuronal cytosol to protrusion.

In the present study, we found that terahertz radiation could change the firing pattern of neurons by decreasing the membrane area ratio of neuronal cytosol and protrusion and decreasing the firing rate and amplitude of action potentials of neurons. Some studies have shown that the firing rate and firing pattern of neuronal action potentials are mainly controlled by the firing threshold [35]. However, the discharge threshold is not a fixed value but is highly variable and highly correlated with neuronal morphology [35, 36]. Decreasing the membrane area ratio of neuronal cytosol and protrusion does not affect the subthreshold activation properties of intracellular Na^+ and K^+ currents. However, it increases the intensity of internal currents between the two intercompartmental compartments of cytosol and protrusion [35]. Since the internal current flows from the cytosol to the protrusion, increasing its strength can result in the cytosol generating a powerful net current flowing out of the cytosol at a subthreshold voltage. This high-intensity hyperpolarizing current drives the cell membrane voltage to a higher value before the Na^+ channels are fully activated, so a higher discharge threshold is generated in the cytosol of the neuron. In addition, the effect of changing the ratio of neuronal cytosol to protruding membrane area is likely caused by the different activation properties of delayed rectifier K^+ currents [35, 37]. Moreover, it has been shown that terahertz radiation of neurons for 15 min can change the concentration of intracellular K^+, but it does not give the pattern of change of K^+ current [24]. Further studies are needed to explain how broadband trace terahertz radiation reduces neuronal firing rate by decreasing the membrane surface and ratio.

Zhao et al. investigated the effect of 3.1 THz radiation on neuronal action potentials and found that the number of neurons generating action potentials increased after terahertz radiation [25]. In this chapter, it was found that terahertz radiation altered the firing pattern of neurons. Although the frequency of inter-cluster discharges of neurons decreased, the frequency of intra-cluster discharges increased. This difference may be related to the terahertz radiation protocol, and neurons responded differently to different radiation protocols, mainly related to the radiation frequency, power, and duration. The present study also found that broadband trace and narrowband high-power terahertz radiation had similar effects on the frequency and amplitude of neuronal inter-cluster and intra-cluster discharges. However, there was a difference in the time of decline of neuronal action potentials. In addition, only a few neuronal discharge kinetic parameters were correlated with the number of terahertz radiation days.

This study found that terahertz radiation can affect synaptic transmission in neurons by decreasing the membrane area ratio of neuronal cytosol and protrusion. The absolute values of postsynaptic current amplitude and falling slope of neurons after radiation increased, and the rise time decreased. To some extent, these parameters reflect physiological properties such as the amount of neurotransmitter release, the number of receptor activations, and the rate of binding and dissociation of receptors from neurotransmitters [38]. An increase in the absolute value of the amplitude of the postsynaptic current can characterize an increase in the amount of neurotransmitter release, the number of receptors, and the number of neurotransmitter-receptor binding [39,40]. This hypothesis is supported by several studies, which have shown that terahertz radiation decreases the content of the inhibitory neurotransmitter GABA and increases the concentration of the excitatory neurotransmitter Glu in neurons [41]. In terms of changes in the number of receptors, it has been found that the number of AMPA receptors increased after radiation. Since excitatory postsynaptic currents mainly comprise AMPA and NMDA mediated currents, the decreasing slopes of the postsynaptic currents correlate strongly with the kinetic properties of AMPA and NMDA receptors [42,43]. The AMPA and NMDA

Journal Pre-proof

receptor-mediated postsynaptic currents differ in time scales, with AMPA-alone-mediated postsynaptic currents typically at 1-3ms reach its peak, whereas NMDA mediated postsynaptic currents alone usually peak at around 10ms [42-45]. Thus, the increase in the absolute value of the slope of the postsynaptic current may be associated with an increase in the proportion of AMPA receptor-mediated postsynaptic currents. Moreover, it has been found that the number of AMPA receptors increased significantly after radiation, but the number of NMDA receptors did not change significantly.

There are also some studies like the findings of this paper. On the experimental side, it has been shown that terahertz radiation increases intracellular Ca^{2+} and Na^{+} concentrations, induces neuronal depolarization, and increases the amplitude of spontaneous excitatory postsynaptic currents [24,25]. At the theoretical level, Guo et al. used BD simulations to study the spontaneous radiation generated by Ca^{2+} movement in calcium channels and the effect of radiation on Ca^{2+} transport. It was found that Ca^{2+} could generate terahertz waves when moving in calcium channels [21]. It was also found that external terahertz radiation can accelerate Ca^{2+} through ion channels and that the acceleration effect is related to the frequency and amplitude of the radiation [21]. These suggest that terahertz radiation can affect the flow of ions by controlling the structure and properties of ionotropic receptors in neurons, which in turn affects the properties of synaptic transmission dynamics in neurons.

Neurodegenerative diseases are characterized by the gradual loss of neuronal morphology and function and the development of new neuromodulation techniques; the study of the regulation of neuronal morphology and function by neuromodulation techniques and the revelation of the coupling relationship between neuronal morphology and function is the basis of intervention in the treatment of neurodegenerative diseases. In this paper, the relative ratio of neuronal cytosol to protruding membrane area was used to characterize the changes in neuronal morphology and the long-term effects of terahertz radiation on neuronal morphology were investigated. It was found that terahertz radiation causes a decrease in the membrane area ratio of neuronal cytosol to protrusion, and this effect begins on day 1 of terahertz radiation and continues until the end of terahertz radiation. Subsequently, by constructing a model of neuronal kinetic properties regulated by terahertz radiation and using the neuronal membrane area ratio as a regulatory factor, we further elucidated the correlation between neuronal morphological changes and kinetic properties after terahertz radiation. It was found that terahertz radiation altered neurons' firing patterns and kinetic properties by decreasing the membrane area ratio of neuronal cytosol and protrusion. In summary, terahertz radiation further affects the kinetic properties of neurons by modulating neuronal morphology, which correlates with the timing of terahertz radiation. These predict that terahertz radiation at specific frequencies and energies could be developed as a novel, molecular-level neuromodulation technique for intervening or treating neuronal degenerative diseases.

Although we have found that terahertz radiation can affect the dynamics of neurons by decreasing the ratio of their membrane area, the regulation mechanisms are unknown. Several studies have shown that the functions of living organisms are closely related to low-frequency terahertz vibrations and that changes in terahertz dynamics determine the functional states of living organisms, such as ion transport and ligand binding. Protein stability and conformational changes can be manipulated by modulating intracellular low-frequency terahertz vibration modes. These also further suggest that terahertz radiation can affect the functional state of living systems by modulating their low-frequency terahertz vibrations. These findings provide strong support for the study of the mechanism of terahertz neurobiological effects. In the study terahertz radiation parameters are important factors affecting neuronal function, however, due to the limitation of the frequency and power of the radiation source, we only investigated the neuronal response to terahertz

Journal Pre-proof

radiation at a single radiation frequency and power. In addition, there may also be long-term effects of terahertz radiation (neuronal function can still be affected after the terahertz radiation ends), however, this study mainly reveals the correlation between neuronal membrane area ratio and discharge after terahertz radiation, so the experiment focuses on the dynamic pattern of neuronal membrane area ratio and discharge characteristics during these three days of terahertz radiation. In the next study, we will try to investigate the response patterns of neurons under different terahertz radiation parameters, and we will further investigate the long-term effects of terahertz stimulation on neurons, which include the effects on neuronal morphology, synaptic transmission, and firing patterns.

MATERIALS AND METHODS

Terahertz radiation system

The terahertz source used in this study was an avalanche diode terahertz source manufactured by TeraSense, with an output frequency of 0.138 THz and an evanescent degree of 8° To make the terahertz radiation source compatible with the neuronal morphology recording system, the output optical path of the terahertz source was optimized, and the experimental platform is shown in Fig.5. Since the terahertz waves emitted from the terahertz radiation source were divergent, a polytetrafluoroethylene (PTFE) terahertz lens (LAT100, Thorlabs, Newton, NJ, USA) was placed at a distance of 100 mm from the source to convert the terahertz waves into parallel waves. Subsequently, a reflector (MAU50-6, Fei Chuang Yida, Beijing, China) was placed 200 mm away from the lens to change the propagation direction of the terahertz radiation so that the terahertz radiation radiated to the neurons from the bottom of the Petri dish. The effective area of the terahertz waves radiating into the Petri dish can be approximated as a circle with a diameter of 14 mm. To allow real-time measurement of the terahertz radiation energy passing through the Petri dish, a 2nd terahertz lens was placed 100 mm away from the Petri dish to focus the terahertz waves to a high-sensitivity pyroelectric detector (RM9-THz, Ophir, Jerusalem, Israel). A chopper was also used to convert the continuous terahertz radiation into 18 Hz pulse waves, and the power of the terahertz radiation was measured by a digital lock-in amplifier and a power meter and uploaded to a computer for display and processing. To be able to regulate the radiation time of the terahertz system, the external trigger modulation technique was integrated into the terahertz source by connecting a signal generator (DG800 Pro, RIGOL, Beijing, China) to the external trigger interface of the terahertz source, and the regulation of the terahertz radiation time and period was realized by adjusting the output parameters of the signal generator.

Journal Pre-proof

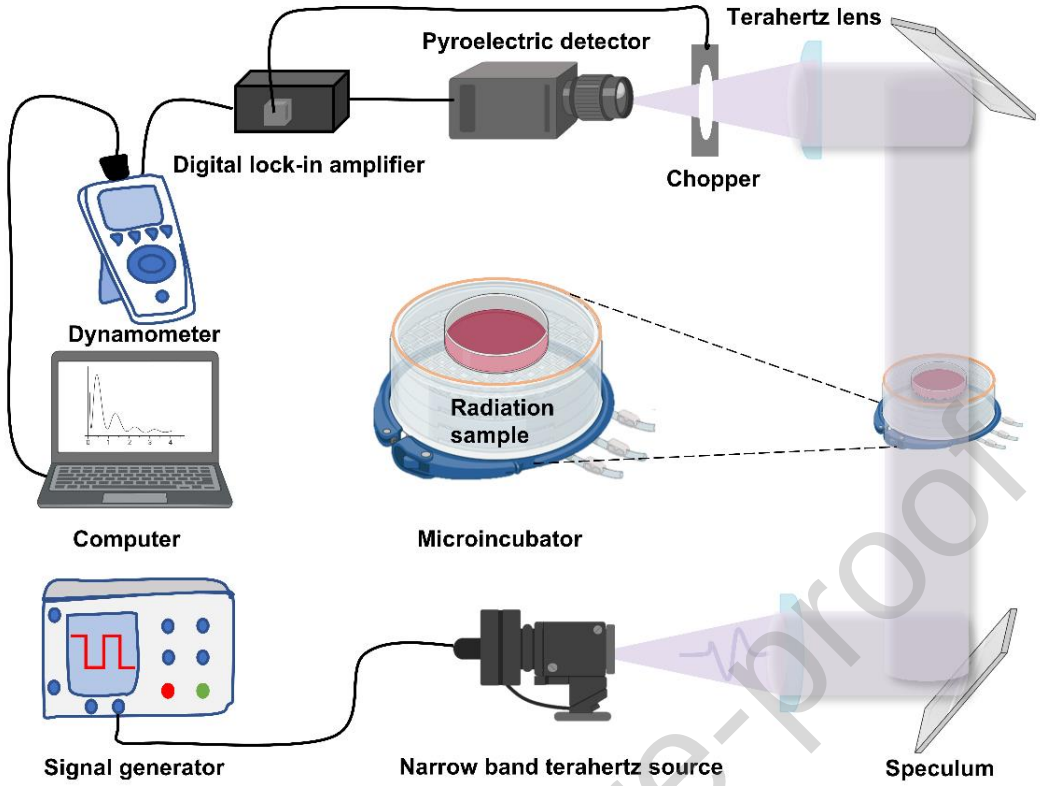


Fig.5. Overall design scheme for a terahertz radiation experimental platform compatible with neuronal morphology recording.

Journal Pre-proof

Primary neuronal culture

Primary neuronal culture was based on Guo's method[46,47], with slight modifications using SPF SD (specific-pathogen-free Sprague-Dawley) pregnant rats, at 12-15 days of gestation, with bodyweight 300-350 g. The fetal rats' cerebral cortexes were extracted in a sterile bench, cut up, added to Trypsin 0.25%, and then digested in an incubator for 15 min and removed every 3 min. Slowly and gently, we blew the neurons with a flame-passivated pasteurized dropper. The cell suspension was grown in 10% fetal bovine serum and 90% Dulbecco's modified eagle medium and adjusted to a concentration of 1 x 10^4 cells in 1 mL. The neurons were then incubated in the incubator for 2 days, and after they had adapted to the environment and grown against the wall, they were irradiated for 20 min per day for 3 days. Since in vitro cultured neurons can be roughly divided into five stages and the duration of each stage is measured in days, it was chosen to utilize terahertz radiation on neurons during the three days of rapid neuronal growth. At the same time, in order to minimize the thermal effect of terahertz radiation, short-time cumulative radiation was used, and the duration of terahertz radiation was 20 min/day for three days, and the morphological changes of neurons were recorded in real time.

Calculation of neuronal membrane area ratio

Neuronal morphology has an important influence on the arrival of electrical signals, in which the membrane area of neuronal cytosol and protrusion is highly correlated with the firing properties of neurons[29]. The calculation of the membrane area ratio of neuronal cytosol to protrusion is divided into four steps: 1) Take pictures of the dynamic growth of neurons before and after terahertz radiation, in which neuronal cytosol and protrusion can be clearly seen, and a representative neuron is shown in Fig. 1(A); 2) The cytosolic radius R_1 and the total length of the protrusion h of the neuron were measured using ImageView

software; 3) Simplify the neuronal morphology by approximating the neuronal cytosol as a sphere with radius R_1 ,where R_1 is the radius of the neuronal cytosol measured in step 2). The neuronal protrusion is approximated as a cylinder with height h and base radius R_2, where h is the total length h of the protrusion measured in step 2), and R_2 is approximated as 5μm (the average radius of the neuronal protrusion), and the simplified model of the neuron is shown in Figure 6;

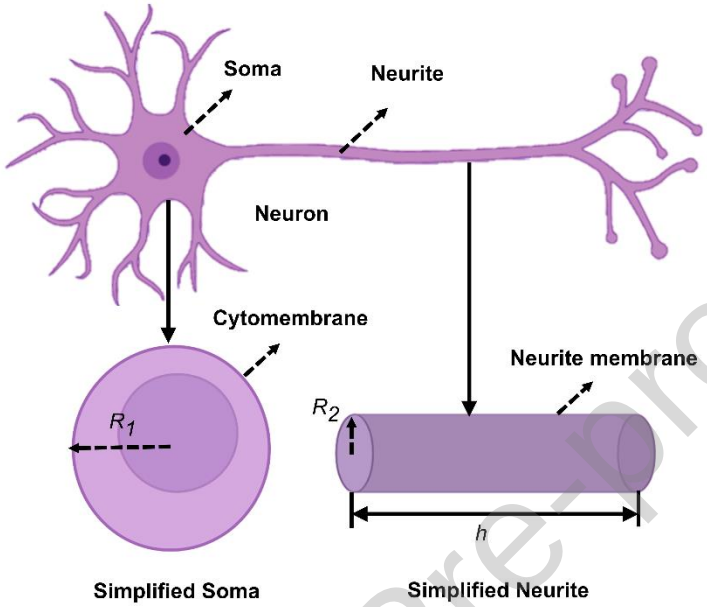


Fig.6. A simplified model of neuronal cytosol and protrusion.

4) Calculate the proportion p of the membrane area between the neuron cell body and the projection, where the membrane area $Area_{body}$ of the neuron cell body is approximately the surface area of a sphere with radius R_1, as shown in equation (1). The membrane area $Area_{neurite}$ of the neurite is approximately the surface area of a cylinder with height h and base radius R_2 (excluding the area of the bottom and top surfaces), and the solution is shown in equation (2). Finally, the ratio of membrane area of neuron body to projection p is the ratio of membrane area of neuron body to total area (membrane area of cell body + projection), and the solution is shown in formula (3).

$$Area_{body} = 4\pi R_1^2 \tag{1}$$

$$Area_{neurite} = 2\pi R_2 h \tag{2}$$

$$p = Area_{body} / \left(Area_{body} + Area_{neurite} \right) \tag{3}$$

Two-compartment pyramidal neuron model

Pyramidal neurons are an important class of excitatory neurons in the brain, and Traub et al. (1991) constructed a computational model of pyramidal neurons in the CA3 region of the hippocampus with 19 intercompartmental compartments based on a large amount of experimental data from voltage-clamp and current-clamp experiments [48]. Subsequently, Pinsky & Rinzel (1994) built a simplified model (PR model) of pyramidal neurons with two inter compartments containing only dendrites and cytosol based on Traub's model. Among them, the PR model can well explain the kinetic properties of CA3 pyramidal neurons, such as cluster discharge and adaptation. In addition, the model is also able to well describe the important role of slow-scale ionic currents distributed on the dendrites of the pyramidal neurons in the generation of cluster discharges[49]. In particular, the PR model is also able to describe well the effect of neuronal morphology on neuronal dynamics.

Journal Pre-proof

The two compartments of the PR neuron model are the cytosol and the dendrites, the structures of which are shown in Fig.7. Among them, the cytosol contains Na+ channels and K+ channels with delayed correction, and the currents of these two ion channels play a key role in the generation of cytosolic action potentials; while in the dendrites contain more ion channels, i.e., Ca^{2+} channels, Ca^{2+} channels with long duration dependent on Ca^{2+}, and K+ channels with short duration dependent on Ca^{2+} and dependent on transmembrane potential, which play an important role in pyramidal neuron cluster discharge, dendritic Ca^{2+} discharge and discharge adaptation[29,48].

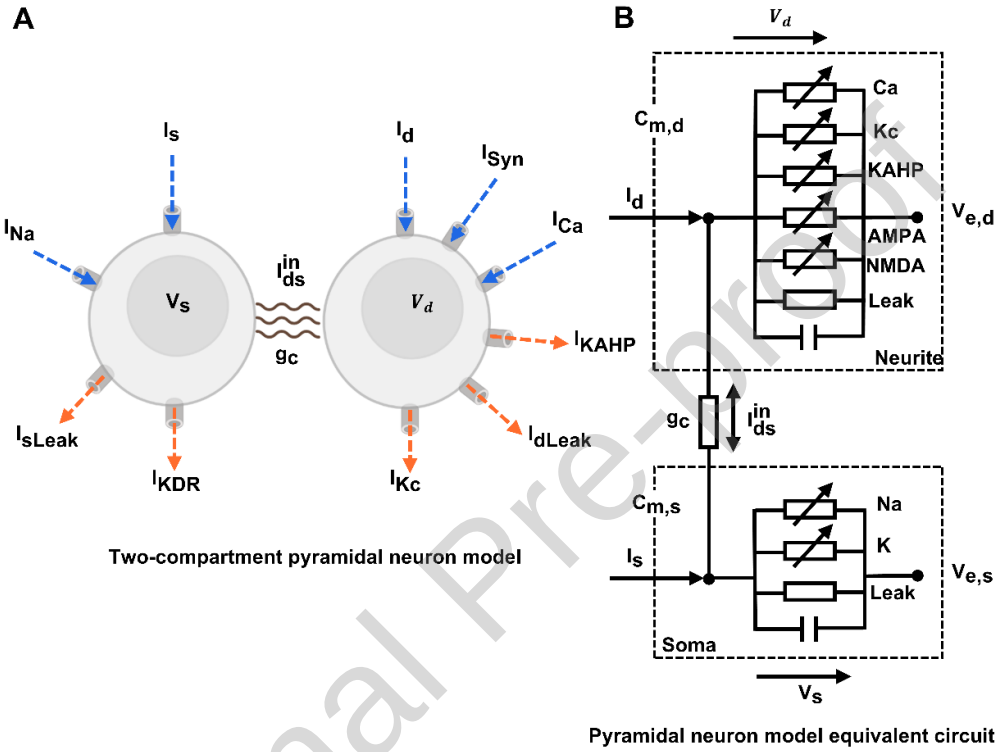


Fig.7. A Modeling of cone neuron dynamics and equivalent circuits in two compartments.

According to the general mathematical model of two-compartment neurons, it is believed that the extracellular space potential will not affect the transmembrane potential of neurons ($V_{e,d} = V_{e,s}$), and the distribution of cell body and dendritic membrane capacitance is the same ($C_{m,d} = C_{m,s}$), then the expression of PR neuron model is as follows[29,50]:

$$\begin{cases} C_m \dfrac{dV_s}{dt} = -I_{sLeak}(V_s) - I_{Na}(V_s,h) - I_{KDR}(V_s,n) + \dfrac{I_{ds}^{in}}{p} + \dfrac{I_s}{p} \\ C_m \dfrac{dV_d}{dt} = -I_{dLeak}(V_d) - I_{Ca}(V_d,s) - I_{KAHP}(V_d,q) - I_{KC}(Vd,Ca,c) - I_{syn} + \dfrac{I_{ds}^{in}}{1-p} + \dfrac{I_d}{1-p} \end{cases} \tag{4}$$

V_s ——Membrane potential of the cytosol;

V_d ——Membrane potential of dendrites;

C_m——Membrane capacitance of cytosol and dendrites;

I_s ——Cytosolic stimulating current;

I_d ——Dendritic stimulating current;

I_{Na} ——Na^+ current;

I_{KDR}——K^+ current with delay correction;

Journal Pre-proof

I_{sLeak} ——Cytosolic leakage current;

I_{Ca} ——Ca^{2+} current;

I_{KAHP} ——Long-term dependence of the K^+ current on Ca^{2+};

I_{KC} ——K+ currents with a short time-course dependence on Ca^{2+} and on transmembrane potentials;

I_{dLeak} ——Dendritic leakage current;

I_{NMDA} ——Synaptic NMDA (N-methyl-D-aspartate) currents;

I_{AMPA} ——Synaptic AMPA currents.

where the membrane area ratio p is.

$$p = \frac{Area_{body}}{Area_{body} + Area_{neurite}} \tag{5}$$

where $Area_{body}$ is the membrane area of the cytosol and $Area_{neurite}$ is the membrane area of the protrusion.

The expression for the coupling current I_{ds}^{in} is:

$$I_{ds}^{in} = g_c\left(V_d - V_s\right) \tag{6}$$

where g_c is the coupled conductance of the cytosol and dendrites, and additionally the ion channel current is defined as[29],[50]:

$$I_{sLeak} = g_L\left(V_s - V_L\right) \tag{7}$$

$$I_{dLeak} = g_L\left(V_d - V_L\right) \tag{8}$$

$$I_{Na} = g_{Na} m_\infty^2 h\left(V_s - V_{Na}\right) \tag{9}$$

$$I_{KDR} = g_{KDR} n\left(V_s - V_K\right) \tag{10}$$

$$I_{KC} = g_{KC} c\chi\left(Ca\right)\left(V_d - V_K\right) \tag{11}$$

$$I_{Ca} = g_{Ca} s^2\left(V_d - V_{Ca}\right) \tag{12}$$

$$I_{KAHP} = g_{KAHP} q\left(V_d - V_K\right) \tag{13}$$

where g_L、g_{Na}、g_{KDR}、g_{KC}、g_{Ca} and g_{KAHP} are the maximum conductance of the corresponding ionic currents, reflecting the density of ion channels distributed across the cell membrane. V_L、V_{Na}、V_K and V_{Ca} denote the equilibrium potentials of the corresponding ionic currents, respectively. Except for I_{sLeak} and I_{dLeak} in cytosol and dendrites, which are passive ion channels, the rest of the ion currents are active ion channels dependent on the gate-change turn-on rate, I_{Na}、I_{KDR}、I_{Ca} are membrane-potential-dependent, I_{KC} are dual-dependent on changes in membrane potential and cytosolic Ca^{2+}concentration, and I_{KAHP} are intracellular Ca^{2+}concentration-dependent. The kinetic equations for the gate variables m、h、n、c、s and q of the active ion channel are[29,50]:

$$\frac{dx}{dt} = \frac{x_\infty - x}{\tau_x}, x = m, h, n, c, s, q \tag{14}$$

Journal Pre-proof

$$x_{\infty}=\frac{\alpha_x}{\left(\alpha_x+\beta_x\right)},\tau_x=\frac{1}{\left(\alpha_x+\beta_x\right)} \tag{15}$$

Of these, descriptions of α_x and β_x are shown in Table 1.

Table 1 Threshold variability function[29,50]

Phylum variable	Pre-rate function	Post-rate function
Na^+channel activation： m	$\alpha_m=\frac{0.32\left(13.1-V_s\right)}{\exp\left(\left(13.1-V_s\right)/4\right)-1}$	$\beta_m=\frac{0.28\left(V_s-40.1\right)}{\exp\left(\left(V_s-40.1\right)/5\right)-1}$
Na^+ channel inactivation： h	$\alpha_h=0.128\exp\left(\frac{17-V_s}{18}\right)$	$\beta_h=\frac{4}{1+\exp\left(\left(40-V_s\right)/5\right)}$
K^+ channel activation： n	$\alpha_n=\frac{0.016\left(35.1-V_s\right)}{\exp\left(\left(35.1-V_s\right)/5\right)-1}$	$\beta_n=0.25\exp\left(0.5-0.025V_s\right)$
Ca^{2+} channel activation： s	$\alpha_s=\frac{1.6}{1+\exp\left(-0.072\left(V_d-65\right)\right)}$	$\beta_s=\frac{0.02\left(V_d-51.1\right)}{\exp\left(\left(V_d-51.1\right)/5\right)-1}$
Concentration-sensitive activation of K^+ channels by Ca^{2+}： c	$\alpha_c=\frac{\exp\left(\left(V_d-10\right)/11-\left(V_d-6.5\right)/27\right)}{18.975}$ $\alpha_c=2\exp\left(\frac{6.5-V_d}{27}\right)$	$\beta_c=2\exp\left(\frac{6.5-V_d}{27}\right)-\alpha_c,V_d\le 50$ $\beta_c=0,V_d>50$
K^+AHP channel activation： q	$\alpha_q=\min\left(0.00002Ca,0.01\right)$	$\beta_q=0.001$

The gate variable $\chi(Ca)$ in I_{KC} depends on the intracellular Ca^{2+} concentration and is expressed as:

$$\chi\left(Ca\right)=\min\left(Ca/250,1\right) \tag{16}$$

The kinetic equation for the intracellular Ca2+ concentration is:

$$\frac{dCa}{dt}=-0.13I_{Ca}-0.075Ca \tag{17}$$

The postsynaptic current is described as:

$$I_{syn}=I_{NMDA}+I_{AMPA} \tag{18}$$

$$I_{NMDA}=g_{NMDA}S_i\left(t\right)\frac{\left(V_d-V_{syn}\right)}{1+0.28\exp\left(-0.062\left(V_d-60\right)\right)} \tag{19}$$

Journal Pre-proof

$$I_{AMPA} = g_{AMPA} W_i(t)\left(V_d - V_{syn}\right) \tag{20}$$

where S_i and W_i denote the NMDA and AMPA-like synaptic conductance weights, respectively, and their kinetic equation expressions are:

$$\begin{cases} \dfrac{dS_i}{dt} = \sum_j H\left(V_{s,j} - 10\right) - \dfrac{S_i}{150} \\ \dfrac{dW_i}{dt} = \sum_j H\left(V_{s,j} - 20\right) - \dfrac{W_i}{2} \end{cases} \tag{21}$$

where $\sum_j$ is summed over all presynaptic neurons; $H(x)$ is the Heaviside step function, viz:

Terahertz stimulation and neuronal models

In order to map the effect of terahertz radiation on neurons to the neuron model, the neuron morphological parameter p was introduced. The morphological parameters of neurons are highly correlated with the firing characteristics of neurons, which can be likened to the relative size of neuronal prominences and cell bodies. When there is a large membrane area ratio in the model, it is similar to the neuron with short prominences, and such a model can generate a tetanic and stable action potential. If the membrane area is relatively small, neurons with longer prominences can be simulated, in which case the model produces a rhythmic action potential. Therefore, the ratio of the membrane area between the cell body and the projection in neurons can be used as a neuroregulatory factor to affect the firing characteristics of neurons. In studying the effect of terahertz radiation on the dynamic properties of neurons, we combine the calculated morphological parameter p with the neuron model. Since the parameter p is calculated based on the morphology of neurons after terahertz radiation, the parameter p has radiation properties. By coupling the parameter p into the neuronal model, the variation of neuronal firing characteristics and postsynaptic current after terahertz radiation can be obtained. The detailed process is as follows:

1) The morphological parameter p of neurons after terahertz radiation was obtained. The calculation method of neuron membrane area ratio p has been given in the previous chapter, and the calculated parameter p has terahertz radiation characteristics (calculated by the morphology of neurons after terahertz radiation);
2) The morphological parameter p with terahertz properties is coupled to the neuron model. The parameter p can be seen from the differential equation of the constructed neuron model, and the parameter p in the model also represents the proportion of the membrane area between the neuron cell body and the projection, as shown in equation (4). Therefore, it is only necessary to bring the parameter p obtained in step 1) into equation (4) to establish a relationship between terahertz radiation and the neuron model.
3) Neuronal action potential and postsynaptic current were calculated after terahertz radiation. By taking the value of neuron morphological parameter p after radiation into equation (4), and solving the equations, we can get the change law of neuron action potential V_s and postsynaptic potential I_{syn} after radiation. Then the intrinsic relationship between parameter p and the firing characteristics of neurons was analyzed.

Quantitative and statistical analysis

Int For statistical analysis of the data, Shapiro-Wilk or Kolmogorov-Smirnov tests for normal distribution were used. All data were expressed as mean ± Standard Error of the Mean. The repeatability of the experiment was characterized by calculating SEM and outliers were detected using Grubbs, special cases are described separately. For datasets that conformed to normal distribution, significant differences were analyzed using independent

Journal Pre-proof

samples t-tests, and when $P < 0.05$, the data were considered significantly different from each other, and statistical plotting was performed using OriginPro.

ACKNOWLEDGMENTS

Author contributions: Conceptualization, X.L. and Y.L.; Data curation, S.L. and H.W.; Formal analysis, S.M. and S.L.; Investigation, S.M. and H.W.; Methodology, C.L. and Y.L.; Resources, X.L.; Modeling, S.M.; Supervision, C.L.; Visualization, S.M.; Writing – original draft, S.M.; Writing – review & editing, C.L., X.L. and Y.L. All authors contributed to the article and approved the submitted version.

Funding: This work was supported by the National Natural Science Foundation of China No. 61827811, Science and Technology Project of Hebei Education Department No. BJ2025013, STI2030 Major Projects No. 2021ZD0204300, Hebei Provincial Military-Civilian Integration Science and Technology Innovation Project of China No. SJMYF202322, Hebei Key Laboratory Project of China No. 202250701010046.

Competing interests: The authors declare that they have no competing financial interests.

DATA AVAILABILITY

Data available on request from the authors. The data that support the findings of this study are available from the corresponding author, Y.L., upon reasonable request.

REFERENCES

[1] Zhang J, Li S, Le W. Advances of Terahertz Technology in Neuroscience: Current Status and a Future Perspective. *iScience*. 2021;24 (12):103548. DOI: 10.1016/j.isci.2021.103548

[2] Cherkasova O, Serdyukov D, Nemova E, Ratushnyak A, Kucheryavenko A, Dolganova I, Xu G, Skorobogatiy M, Reshetov I, Timashev, et al. Cellular Effects of Terahertz Waves. *Journal of Biomedical Optics*. 2021; 26 (9): 090902.DOI: 10.1117/1.JBO.26.9.090902

[3] Mancini T, Mosetti R, Marcelli A, Petrarca M, Lupi S, D'Arco. Terahertz Spectroscopic Analysis in Protein Dynamics: Current Status. *Radiation*. 2022; 2 (1): 100-123. DOI: 10.3390/radiation2010008

[4] Sun L, Zhao L, Peng R. Research Progress in the Effects of Terahertz Waves on Biomacromolecules. *Military Medical Research*. 2021; 8 (1): 28. DOI: 10.1186/s40779-021-00321-8

[5] Niessen K, Xu M, George D, Chen M, Ferré-D'Amaré A, Snell E, Cody V, Pace J, Schmidt M, Markelz A. Protein and RNA Dynamical Fingerprinting. *Nature Communications*. 2019; 10 (1): 1026. DOI: 10.1038/s41467-019-08926-3

[6] Varvdekar B, Prabhakant A, Krishnan M. Response of Terahertz Protein Vibrations to Ligand Binding: Calmodulin-Peptide Complexes as a Case Study. *Journal of Chemical Information and Modeling*. 2022; 62 (7): 1669-1679. DOI: 10.1021/acs.jcim.1c01344

[7] Li Y, Chang C, Zhu Z, Sun L, Fan C. Terahertz Wave Enhances Permeability of the Voltage-Gated Calcium Channel. *Journal of the American Chemical Society*. 2021; 143 (11): 4311-4318. DOI: 10.1021/jacs.0c09401

[8] Castro-Camus E, Johnston M. Conformational Changes of Photoactive Yellow Protein Monitored by Terahertz Spectroscopy. *Chemical Physics Letters*. 2008; 455 (4-6): 289-292. DOI: 10.1016/j.cplett.2008.02.084

[9] Adams E, Pezzotti S, Ahlers J, Rüttermann M, Levin M, Goldenzweig A, Peleg Y, Fleishman S, Sagi I, Havenith M. Local Mutations Can Serve as a Game Changer for

Journal Pre-proof

Global Protein Solvent Interaction. *JACS Au*. 2021; 1 (7): 1076-1085. DOI: 10.1021/jacsau.1c00155
[10] Fischer B, Walther M, Uhd Jepsen P. Far-Infrared Vibrational Modes of DNA Components Studied by Terahertz Time-Domain Spectroscopy. *Physics in Medicine and Biology*. 2002; 47 (21): 3807-3814. DOI: 10.1088/0031-9155/47/21/319
[11] Cherkasova O, Fedorov V, Nemova E, Pogodin S. Influence of Terahertz Laser Radiation on the Spectral Characteristics and Functional Properties of Albumin. *Optics and Spectroscopy*. 2009; 107 (4): 534-537. DOI: 10.1134/s0030400x09100063
[12] Lundholm I, Rodilla H, Wahlgren W, Duelli A, Bourenkov G, Vukusic J, Friedman R, Stake J, Schneider T, Katona G. Terahertz Radiation Induces Non-thermal Structural Changes Associated with Fröhlich Condensation in a Protein Crystal. *Structural Dynamics*. 2015; 2(5): 054702. DOI: 10.1063/1.4931825
[13] Ma S, Ding P, Zhou Z, Jin H, Li X, Li Y. Terahertz Radiation Modulates Neuronal Morphology and Dynamics Properties. *Brain Sci*. 2024; 14: 279. DOI: 10.3390/brainsci14030279
[14] Ma S, Li Z, Gong S, Lu C, Li X, Li Y. High Frequency Electromagnetic Radiation Stimulates Neuronal Growth and Hippocampal Synaptic Transmission. *Brain Sci*. 2023; 13: 686. DOI: 10.3390/brainsci13040686
[15] Ma S, Li Z, Gong S, Lu C, Li X, Li Y. The laws and effects of terahertz wave interactions with neurons. *Front. Bioeng. Biotechnol*. 2023; 11:1147684. DOI: 10.3389/fbioe.2023.1147684
[16] Ma S, Gong S, Zhang W, Lu C, Li X, Li Y. Neuronal growth and development promoted by low-intensity roadband terahertz radiation. *Acta Phys. Sin*. 2022; 71(20): 208701. DOI: 10.7498/aps.71.20220636
[17] Zhao L, Yi R, Liu S, Chi Y, Tan S, Dong J, Wang H, Xu X, et al. Biological Responses to Terahertz Radiation with Different Power Density in Primary Hippocampal Neurons. *PLoS One*. 2023; 18(1): e0267064. DOI: 10.1371/journal.pone.0267064
[18] Sulatsky M, Duka M, Smolyanskaya O. Stimulation of Neurite Growth Under Broadband Pulsed THz Radiation. *Physics of Wave Phenomena*. 2014; 22 (3): 197-201. DOI: 10.3103/s1541308x14030066
[19] Duka M, Dvoretskaya L, Babelkin N, Khodzitskii M, Chivilikhin S, Smolyanskaya O. Numerical and Experimental Studies of Mechanisms Underlying the Effect of Pulsed Broadband Terahertz Radiation on Nerve Cells. *Quantum Electronics*. 2014; 44 (8): 707-712. DOI: 10.1070/qe2014v044n08abeh015486
[20] Tsurkan M, Smolyanskaya O, Bespalov V, Penniyainen V, Kipenko A, Lopatina E, Krylov B. Changing Growth of Neurites of Sensory Ganglion by Terahertz Radiation. *Proceedings of SPIE-The International Society for Optical Engineering*. 2012; 8261: 23. DOI: 10.1117/12.909350
[21] Guo L, Bo W, Wang K, Wang S, Gong Y. Theoretical Investigation on the Effect of Terahertz Wave on Ca^{2+} Transport in the Calcium Channel. *iScience*. 2021;25(1): 103561.DOI: 10.1016/j.isci.2021.103561
[22] Sun S, Titushkin I, Varner J, Cho M. Millimeter Wave-Induced Modulation of Calcium Dynamics in an Engineered Skin Co-culture Model: Role of Secreted ATP on Calcium Spiking. *Journal of Radiation Research*. 2012; 53(2): 159-167.DOI: 10.1269/jrr.11037
[23] Titushkin I, Rao V, Pickard W, Moros E, Shafirstein G, Cho M. Altered Calcium Dynamics Mediates P19-Derived Neuron-Like Cell Responses to Millimeter-Wave Radiation. Radiation Research. 2009; 172(6): 725-736.DOI: 10.1667/RR1760.1
[24] Zhang X, He M, Zhao J, Chen X, Liu L, Lu X, Tian T, Chen M, Wang P. Effect of 0.1 THz Radiation on Excitability of Hippocampal Neurons in Sprague Dawley Rats. *Chinese Journal of Lasers*. 2020; 47(2): 0207023.DOI: 10.3788/cjl202047.0207023

Journal Pre-proof

[25] Zhao X, Zhang M, Liu Y, Liu H, Ren K, Xue Q, Zhang H, Zhi N, Wang W, Wu S. Terahertz Exposure Enhances Neuronal Synaptic Transmission and Oligodendrocyte Differentiation in Vitro. *iScience*. 2021; 24 (12): 103485.DOI: 10.1016/j.isci.2021.103485
[26] Longhena F, Faustini G, Brembati V, Pizzi M, Benfenati F, Bellucci A. An updated reappraisal of synapsins: structure, function and role in neurological and psychiatric disorders. *Neuroscience & Biobehavioral Reviews*. 2021; 130: 33-60. DOI: 10.1016/j.neubiorev.2021.08.011
[27] EL-Andari R, Cunha F, Tschirren B, Iwaniuk A. Selection for Divergent Reproductive Investment Affects Neuron Size and Foliation in the Cerebellum. *Brain Behav Evol*. 2020; 95 (2): 69–77.DOI: 10.1159/000509068
[28] Lui J, Hansen D, Kriegstein A. Development and Evolution of the Human Neocortex. *Cell*. 2011; 146(1): 18-36.DOI: 10.1016/j.cell.2011.06.030
[29] Wei X, Wang J, Yu H. Nervous system modeling and control engineering. *Beijing: Science Press*. 2015; 40-80.
[30] Berzhanskaya J, Chernyy N, Gluckman B, Schiff S, Ascoli G. Modulation of Hippocampal Rhythms by Subthreshold Electric Fields and Network Topology. *Journal of Computational Neuroscience*. 2012; 34(3): 369-389.DOI: 10.1007/s10827-012-0426-4
[31] Radman T, Ramos R, Brumberg J, Bikson M. Role of Cortical Cell Type and Morphology in Subthreshold and Suprathreshold Uniform Electric Field Stimulation in Vitro. *Brain Stimulation*. 2009; 2(4): 215-228.DOI: 10.1016/j.brs.2009.03.007
[32] Pinsky P, Rinzel J. Intrinsic and Network Rhythmogenesis in a Reduced Traub Model for CA3 Neurons. *Journal of Computational Neuroscience*. 1994; 1(1-2): 39-60.DOI: 10.1007/BF00962717
[33] Tchuisseuh M, Chamgoué A, Kakmeni F. Effect of the electromagnetic induction in the electrical activity of the Kazantsev model of inferior Olive Neuron model. Biosystems. 2015; 236:105114. DOI: 10.1016/j.biosystems.2023.105114
[34] Zha C. Study on the mechanism of CRMP2 and CRMP4 regulating the axon development of hippocampal neurons. *Guangzhou: Doctoral Dissertation of Jinan University*. 2016; 12-36. DOI: 10.1016/j.biosystems.2023.105114
[35] Yi G, Zhao Q, Wei X, Wang J. Variability and Significance of Spike Threshold in Neurons. *Progress in Biochemistry and Biophysics*. 2022; 49(07): 1226-1242. DOI: 10.16476/j.pibb.2021.0255
[36] Yi G, Wang J, Wei X, Deng B. Dynamics of Spike Threshold in a Two-Compartment Neuron with Passive Dendrite. *Communications in Nonlinear Science and Numerical Simulation*. 2016; 40: 100-111.DOI: 10.1016/j.cnsns.2016.04.021
[37] Goethals S, Brette R. Theoretical Relation Between Axon Initial Segment Geometry and Excitability. *eLife*. 2020; 9: e53432. DOI: 10.1016/j.cnsns.2016.04.021
[38] Wang B, Dudko O. A Theory of Synaptic Transmission. *eLife*. 2021; 10: e73585. DOI: 10.7554/eLife.73585
[39] Statman A, Kaufman, M, Minerbi A, Ziv A, Brenner N. Synaptic Size Dynamics as an Effectively Stochastic Process. *PLoS Computational Biology*. 2014; 10(10): e1003846. DOI: 10.1371/journal.pcbi.1003846
[40] Wagner T, Valero-Cabre A, Pascual-Leone A. Noninvasive Human Brain Stimulation. *Annual Review of Biomedical Engineering*. 2007; 9: 527-565.DOI: 10.1146/annurev.bioeng.9.061206.133100
[41] Sun L, Chen M, Wang H, Dong J, Zhao L. Peng R. CaMKIIδ Promotes Synaptic Plasticity under Terahertz Wave Radiation by Activation of the NF-κB Pathway. *Journal of Physical Chemistry Letters*. 2022; 13(25): 5925-5931.DOI: 10.1021/acs.jpclett.2c00775

Journal Pre-proof

[42] Anggono V, Huganir R. Regulation of AMPA Receptor Trafficking and Synaptic Plasticity. *Current Opinion Neurobiology*. 2012; 22(3): 461-469.DOI: 10.1016/j.conb.2011.12.006

[43] Hu E, Bouteiller J, Huang M, Dong S, Berger T. A Comparison Between Direct and Indirect Measurements of Neurotransmitter Vesicle Release Dynamics: a computational study. *2014 36th Annual International Conference of the IEEE Engineering in Medicine and Biology Society, Chicago, IL, USA*. 2014; 1155-1158. DOI: 10.1109/EMBC.2014.6943800

[44] Bouteiller J, Baudry M, Allam S, Greget R, Bischoff S. Modeling Glutamatergic Synapses: Insights into Mechanisms Regulating Synaptic Efficacy. *Journal of Integrative Neuroscience*. 2008; 7(2): 185-197.DOI: 10.1142/s0219635208001770

[45] Abrahamsson T, Chou C, Li S, Mancino A, Costa R, Brock J, Nuro E, Buchanan K, Elgar D, Blackman A, et al. Differential Regulation of Evoked and Spontaneous Release by Presynaptic NMDA Receptors. Neuron. 2017; 96(4): 839-855. DOI: 10.1016/j.neuron.2017.09.030

[46] Guo Z, Li C, Li X, Wang Y. Mattson M, Lu C. The developmental regulation of glutamate receptor-mediated calcium signaling in primary cultured rat hippocampal neurons. Neuroreport. 2013; 24:492-497. DOI:10.1097/WNR.0b013e32836206b5

[47] Goshi N, Kim H, Girardi G, Gardner A. Seker, E. Electrophysiological Activity of Primary Cortical Neuron-Glia Mixed Cultures. Cells. 2023; 12(5):821. DOI:10.3390/cells12050821

[48] Traub R, Wong R, Miles R, Michelson H. A Model of a CA3 Hippocampal Pyramidal Neuron Incorporating Voltage-Clamp Data on Intrinsic Conductances. *Journal of Neurophysiology*. 1991; 66(2): 635-650.DOI: 10.1152/jn.1991.66.2.635

[49] Sætra M, Einevoll G, Halnes G. An electrodiffusive, ion conserving Pinsky-Rinzel model with homeostatic mechanisms. *Plos Comput Biol*. 2020; 16(4): e1007661.DOI: 10.1371/journal.pcbi.1007661

[50] Park E, Barreto E, Gluckman B, Schiff S, So P. A model of the Effects of Applied Electric Fields on Neuronal Synchronization. *Journal of Computational Neuroscience*. 2005; 19(1): 53-70.DOI: 10.1007/s10827-005-0214-5

Journal Pre-proof

Author Statement

Conceptualization, X.L. and Y.L.; Data curation, S.L. and H.W.; Formal analysis, S.M. and S.L.; Investigation, S.M. and H.W.; Methodology, C.L. and Y.L.; Resources, X.L.; Modeling, S.M.; Supervision, C.L.; Visualization, S.M.; Writing – original draft, S.M.; Writing – review & editing, C.L., X.L. and Y.L. All authors contributed to the article and approved the submitted version.

Journal Pre-proof

Declaration of Interest Statement

The authors declare that they have no known competing financial interests or personal relationships that could have appeared to influence the work reported in this paper.

Journal Pre-proof

Highlights

- Terahertz radiation caused a decrease in the membrane area ratio of neuronal cytosol to protrusion, and this effect started on the first day of terahertz radiation and lasted until the end of terahertz radiation;

- Terahertz radiation can modulate neurons' morphology and change their firing patterns and kinetic properties by affecting their morphology.

Journal Pre-proof